Supplement of The Cryosphere, 14, 2977–2997, 2020
https://doi.org/10.5194/tc-14-2977-2020-supplement

The Cryosphere Open Access EGU

Supplement of

Seasonal transition dates can reveal biases in Arctic sea ice simulations

Abigail Smith et al.

Correspondence to: Abigail Smith (abigail.l.smith@colorado.edu)

625 **Supplementary Material**

Citations	Date range	Timing	Threshold	Consecutive Days
Break-up				
Bliss et al. (2019); Steele et al. (2019)	1 March to SIC minimum date	last day	below 15%	–
Serreze et al. (2016)	*X*	first day	below 30%	–
Stammerjohn et al. (2008, 2012)	mid-September to mid-September	last day	below 15%	–
Stroeve et al. (2016)	1 March to SIC minimum date	last day	below 15, 30, 50%	–
Wang et al. (2018)	1 March and 30 September	first day	below 15%	2
Freeze-up				
Bliss et al. (2019); Steele et al. (2019)	SIC minimum date to 28 February	first day	above 15%	–
Serreze et al. (2016)	SIC minimum date to *X*	first day	above 30%	–
Stammerjohn et al. (2008, 2012)	mid-September to mid-September	first day	above 15%	5
Stroeve et al. (2016)	SIC minimum date to 28/29 February	first day	above 15, 30, 50%	–
Wang et al. (2018)	1 September to 31 March	first day	above 15%	2
Open water period				
Barnhart et al. (2016)	11 March to 11 March	number of days	below 15%	–

Table S1. Definitions for break-up (retreat), freeze-up (advance) and the open water period. All studies in the table except Barnhart et al. (2016) calculate the open water period as the number of days between break-up and freeze-up. Information designated with *X* is not provided in the cited manuscripts.

Model	Ocean model	Sea ice model	Ice-ocean Resolution (latitude x longitude)	Citations
ACCESS-CM2	MOM5	CICE5	primarily 1°x 1°	Dix et al. (2019)
BCC-CSM2-MR	MOM4	SIS2	0.3-1°x 1°	Wu et al. (2018, 2019)
BCC-ESM1	MOM4	SIS2	0.3-1°x 1°	Zhang et al. (2018); Wu et al. (2019)
CanESM5	NEMO3.4.1 ORCA1	LIM2	0.3-1°x 1°	Swart et al. (2019a, b)
CESM2	POP2	CICE5	0.9°x 1.25°	Danabasoglu (2019a); DeRepentigny et al. (2020)
CESM2-FV2	POP2	CICE5	0.9°x 1.25°	Danabasoglu (2019b)
CESM2-WACCM	POP2	CICE5	0.9°x 1.25°	Danabasoglu (2019c) DeRepentigny et al. (2020)
CESM2-WACCM-FV2	POP2	CICE5	0.9°x 1.25°	Danabasoglu (2019d)
CNRM-ESM2-1	NEMO3.6 eORCA1	GELATO6	primarily 1°x 1°	Seferian (2018); Voldoire et al. (2019)
CNRM-CM6-1	NEMO3.6 eORCA1	GELATO6	primarily 1°x 1°	Voldoire (2018); Voldoire et al. (2019)
EC-Earth3	NEMO3.6 eORCA1	LIM3	0.3-1°x 1°	EC-Earth-Consortium (2019);
IPSL-CM6A-LR	NEMO-OPA eORCA1.3	LIM3	~1°x ~1°	Boucher et al. (2018, 2020)
MRI-ESM2-0	MRI.COM4.4	MRI.COM4.4	0.3-0.5°x 1°	Yukimoto et al. (2019a, b)
NorESM2-LM	MICOM	CICE5	primarily 1°x 1°	NCC (2018a); Seland et al. (submitted 2020)
NorESM2-MM	MICOM	CICE5	primarily 1°x 1°	NCC (2018b); Seland et al. (submitted 2020)
CESM LE	POP2	CICE4	0.3-1°x 1°	Hurrell et al. (2013); Kay et al. (2015)

Table S2. Ocean and sea ice models used by the coupled models, as well as their primary ice-ocean resolutions and associated citations.

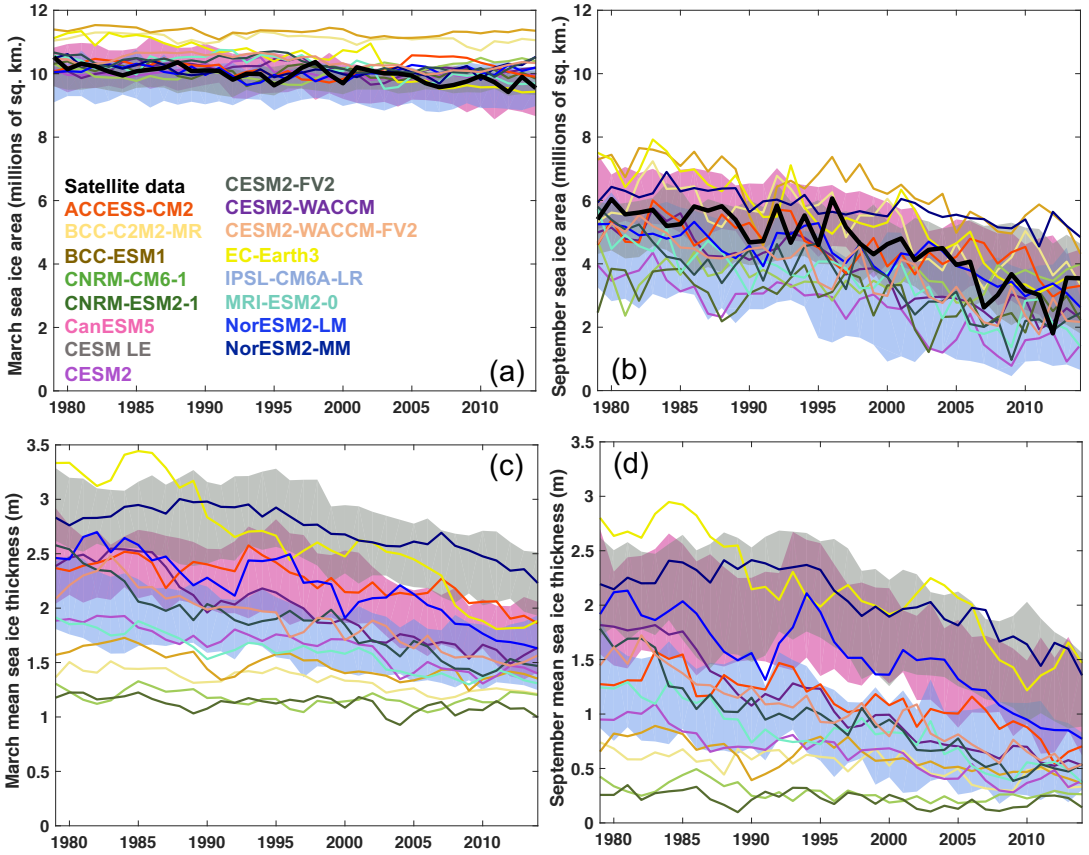

Figure S1. From 1979–2014, (a) March sea ice area (b) September sea ice area (c) March mean ice thickness and (d) September mean ice thickness in CMIP6 models (various colors), CESM LE (gray) and satellite observations (black) in the Arctic. All ensemble members are shown for CESM (40 members), CanESM5 (35 members) and IPSL (30 members). Metrics are averaged from 66-84.5°N and observations of sea ice thickness are not shown.

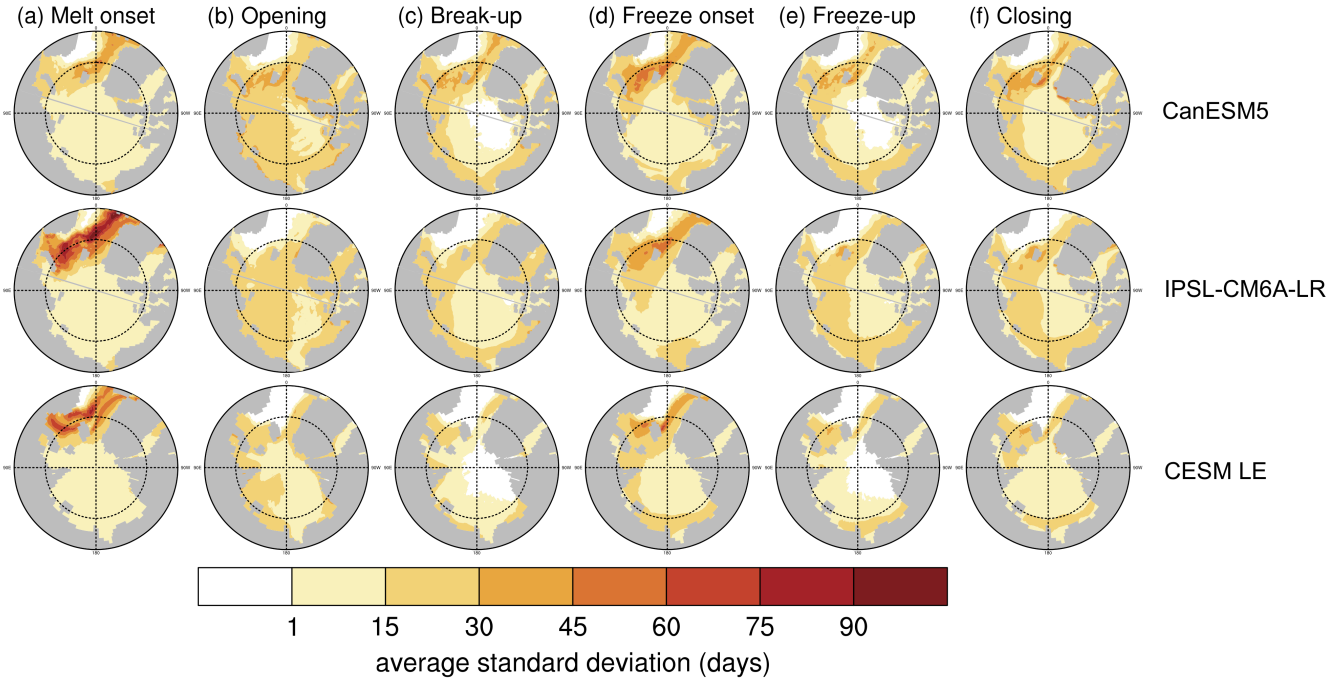

Figure S2. The average standard deviation between all available ensemble members over 1979–2014 for (a) melt onset (b) opening (c) break-up (d) freeze onset (e) freeze-up (f) closing. CanESM5 is displayed in the first row (35 members), IPSL is displayed in the second row (30 members) and CESM LE is displayed in the third row (40 members). The standard deviation is calculated at each grid cell for each year, and then the average of all years is plotted for each grid cell. The same figure using the first 30 ensemble members of each model is displayed in Fig. 8.

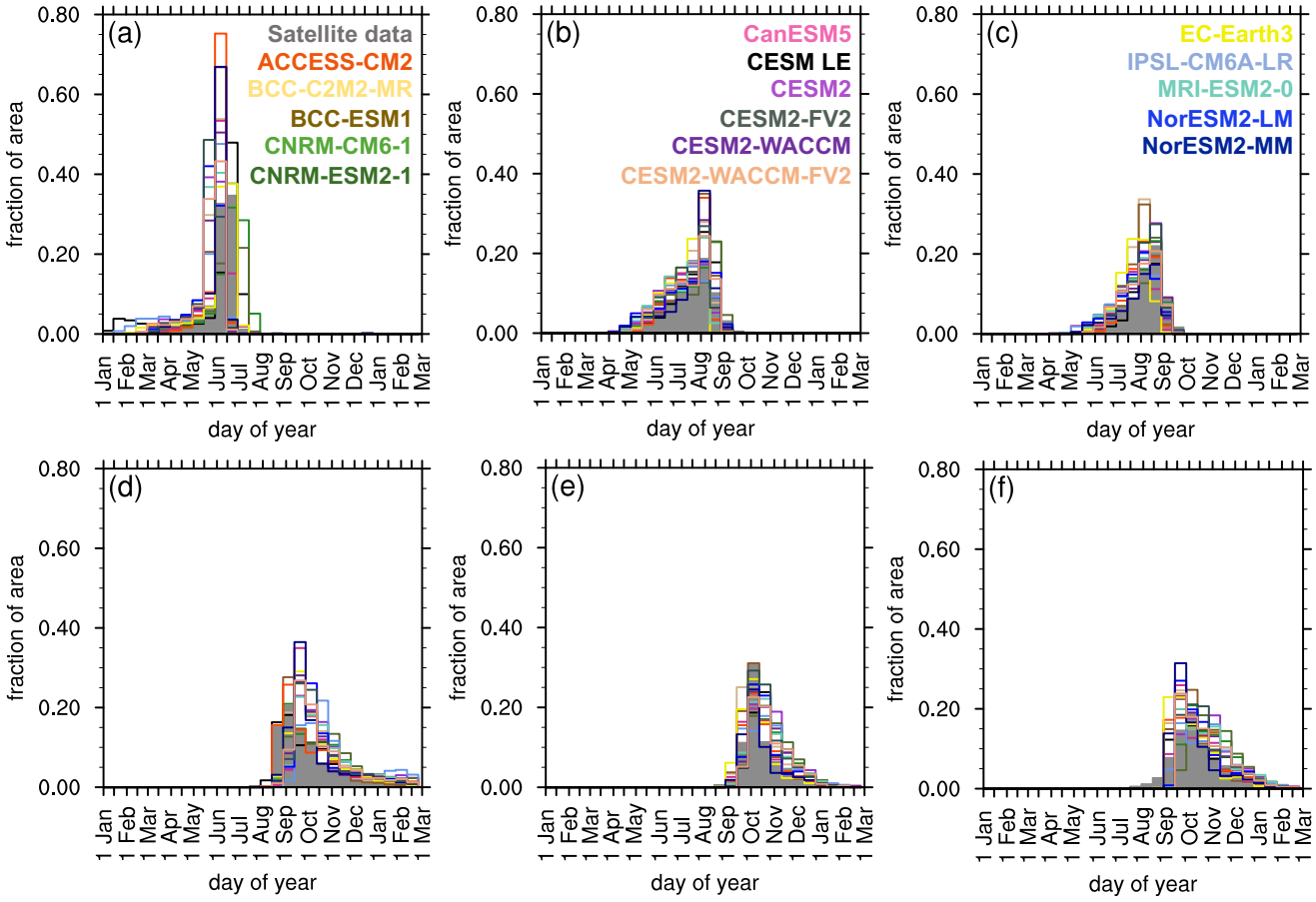

Figure S3. Area distributions of the average of each metric from 1979–2014: (a) melt onset (b) opening (c) break-up (d) freeze onset (e) freeze-up and (f) closing. Metrics are averaged from 66-84.5°N for satellite data (filled gray) and the first ensemble member of each model (all other colors). All models and satellite data are represented in each panel (a)-(f), but the color labels are distributed across panels (a)-(c).

	Melt onset	Opening (80%)	Break-up (15%)	Freeze onset	Freeze-up (15%)	Closing (80%)
ACCESS-CM2	12	24	19	48	24	30
BCC-CSM2-MR	18	25	18	31	22	30
BCC-ESM1	17	24	18	30	21	27
CanESM5	18	28	26	41	29	35
CESM2	22	27	23	42	26	32
CESM2-FV2	18	26	22	41	24	29
CESM2-WACCM	21	27	23	40	25	31
CESM2-WACCM-FV2	21	28	24	39	25	31
CNRM-ESM2-1	24	32	28	48	26	30
CNRM-CM6-1	25	31	27	47	26	30
EC-Earth3	29	23	20	36	22	28
IPSL-CM6A-LR	36	31	29	43	29	34
MRI-ESM2-0	19	28	26	42	26	32
NorESM2-LM	20	34	27	39	24	30
NorESM2-MM	22	32	27	39	26	30
CESM LE	47	26	19	48	23	31
Satellite data	20	32	27	44	27	36

Table S3. Satellite-era (1979–2014) spatial standard deviations across the Arctic (in days, between 66-84.5°N) of seasonal sea ice transition dates calculated using the satellite data and the first ensemble member from each model.

	Melt period	**Seasonal loss-of-ice period**	**Freeze period**	**Seasonal gain-of-ice period**	**Melt season**	**Open water period**	**Outer ice-free period**
ACCESS-CM2	18	9	8	7	49	41	52
BCC-CSM2-MR	17	12	7	7	47	39	53
BCC-ESM1	20	13	7	7	44	37	49
CanESM5	16	10	7	6	49	54	61
CESM2	21	8	7	7	59	46	56
CESM2-FV2	21	10	6	6	54	43	52
CESM2-WACCM	22	10	6	8	57	45	55
CESM2-WACCM-FV2	22	10	7	6	57	46	57
CNRM-ESM2-1	21	7	6	6	63	52	60
CNRM-CM6-1	18	8	8	5	63	50	60
EC-Earth3	17	10	12	8	59	40	51
IPSL-CM6A-LR	22	8	15	5	71	55	62
MRI-ESM2-0	20	11	7	7	56	49	60
NorESM2-LM	24	10	9	6	54	48	61
NorESM2-MM	19	14	9	7	52	51	61
CESM LE	16	12	14	10	83	39	56
Satellite data	21	12	29	10	58	49	61

Table S4. Satellite-era (1979–2014) spatial standard deviations across the Arctic (in days, between 66-84.5°N) of intra-seasonal periods (melt period, seasonal loss-of-ice period, freeze period and seasonal gain-of-ice period) and inter-seasonal periods (melt season, open water period and outer ice-free period) calculated using the satellite data and the first ensemble member from each model.

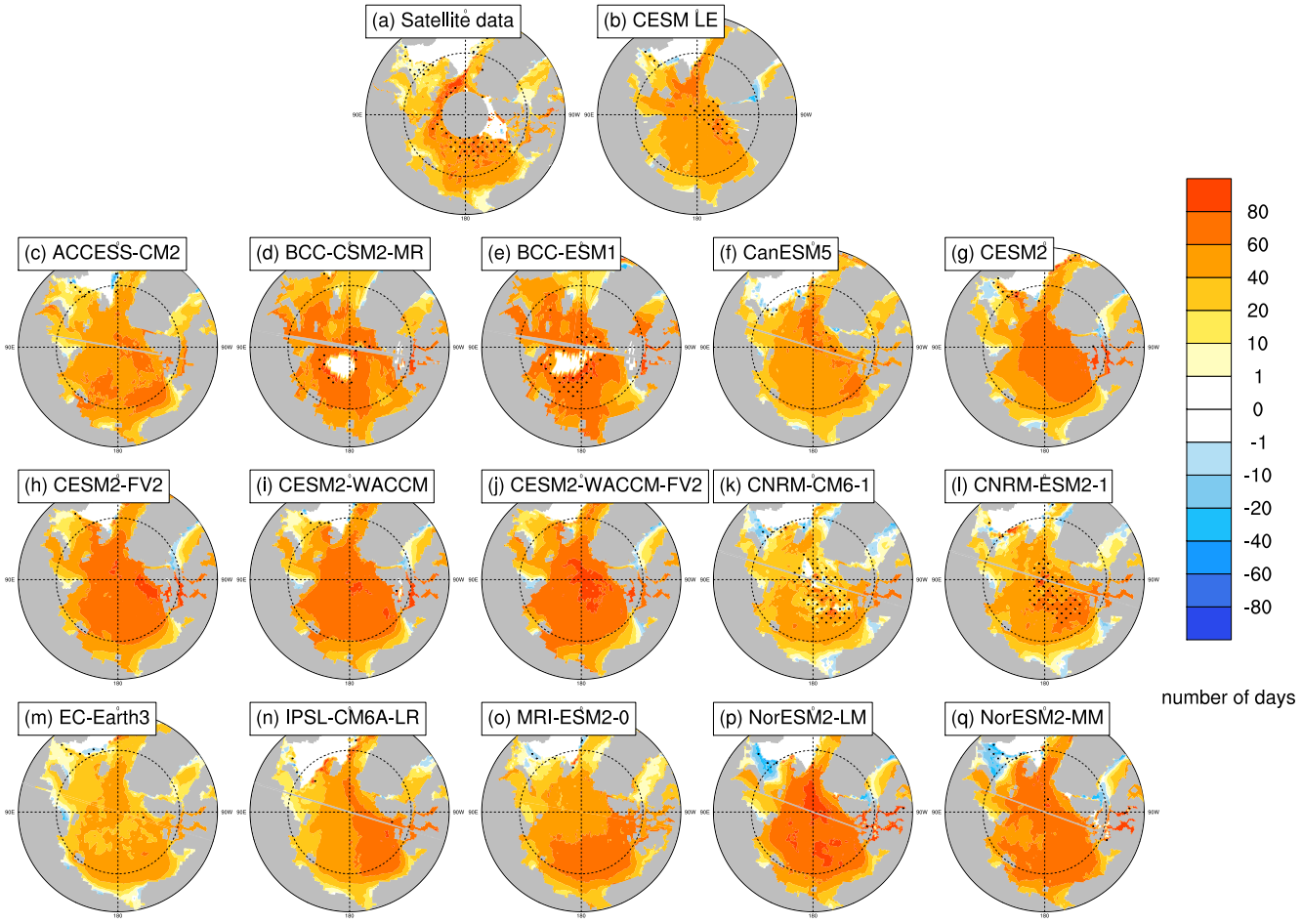

Figure S4. The length of the melt period (number of days between melt onset and opening) averaged over 1979–2014 at each grid cell using satellite data (a), the first ensemble member of the CESM LE (b) and the first ensemble member of each CMIP6 model (c-q). Stippling indicates where closing dates exist in less than 20% of years in the time range. Models on tripolar grids produce plot gaps filled by gray lines. Negative values indicate where the opening date falls earlier than the melt onset. This can occur due to physical reasons (i.e., dynamical ice divergence or bottom melt), or due to the fact that melt onset is defined using surface temperature and opening is defined using ice concentration.

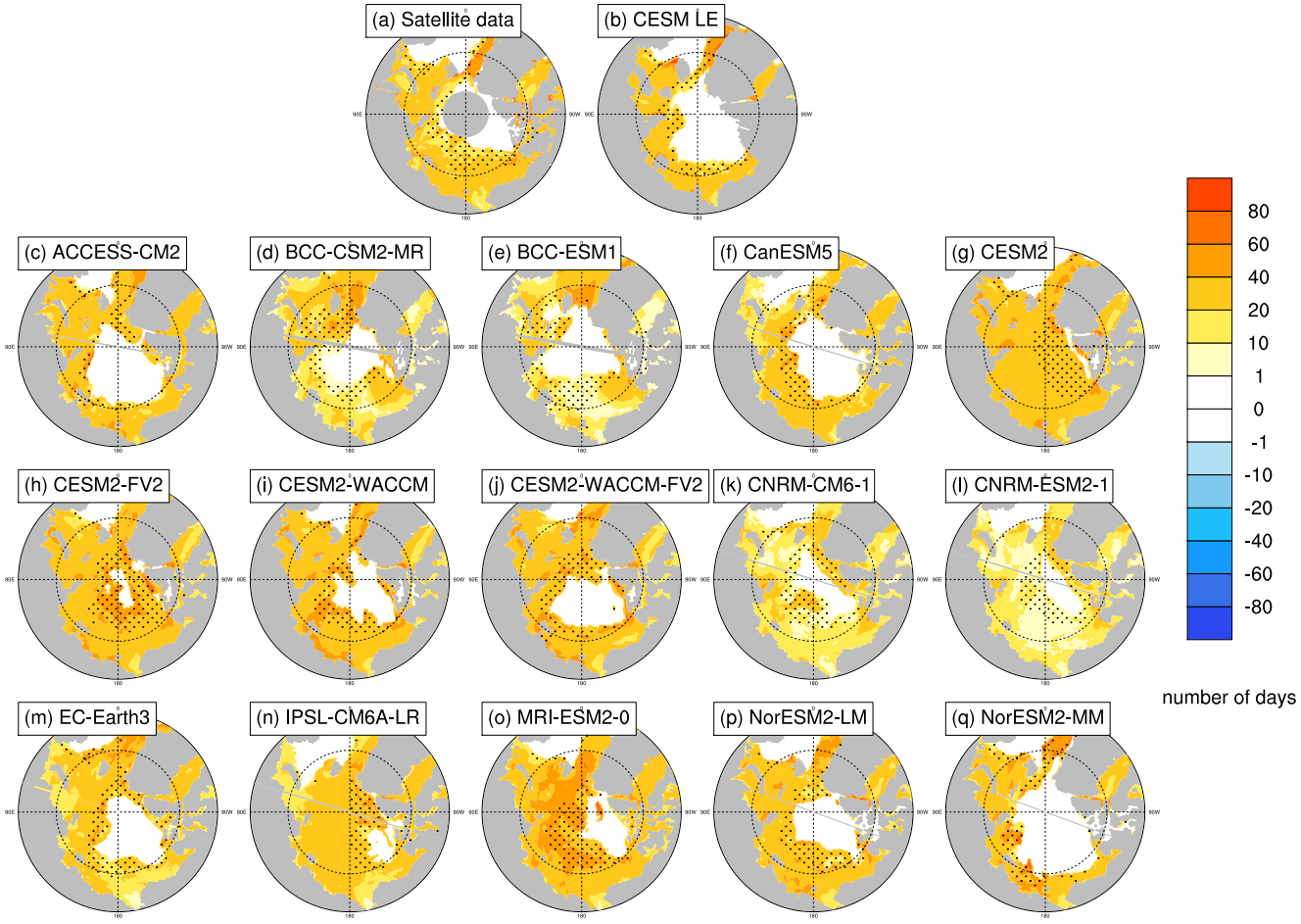

Figure S5. The length of the seasonal loss-of-ice period (number of days between opening and break-up) averaged over 1979–2014 at each grid cell using satellite data (a), the first ensemble member of the CESM LE (b) and the first ensemble member of each CMIP6 model (c-q). Stippling indicates where closing dates exist in less than 20% of years in the time range. Models on tripolar grids produce plot gaps filled by gray lines. No negative values are possible as both metrics are based on sequential ice concentration thresholds (80% and 15%).

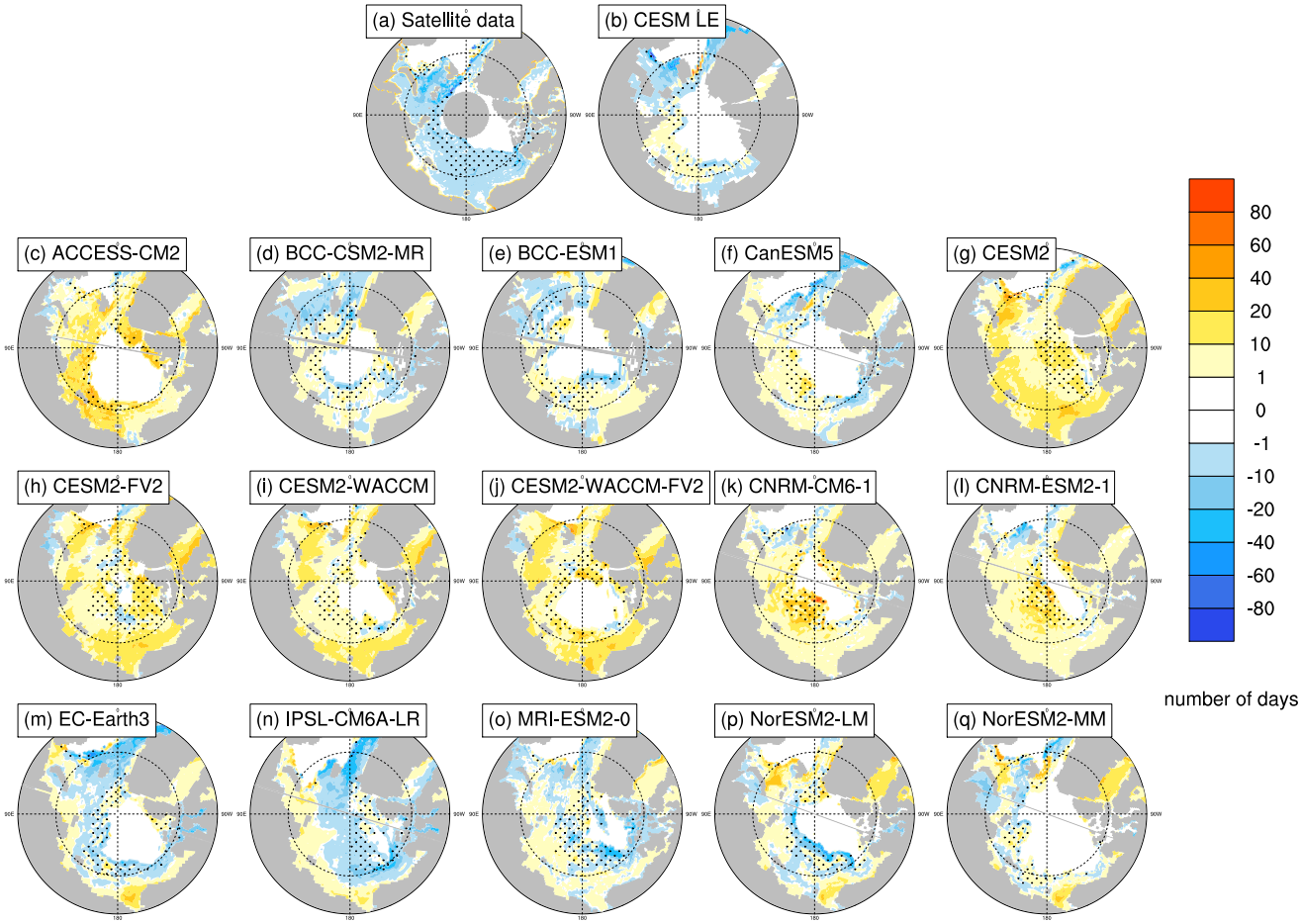

Figure S6. The length of the freeze period (number of days between freeze onset and freeze-up) averaged over 1979–2014 at each grid cell using satellite data (a), the first ensemble member of the CESM LE (b) and the first ensemble member of each CMIP6 model (c-q). Stippling indicates where closing dates exist in less than 20% of years in the time range. Models on tripolar grids produce plot gaps filled by gray lines. Negative values indicate where the freeze-up date falls earlier than the freeze onset. This can occur due to physical reasons (i.e., dynamical ice convergence), or due to the fact that freeze onset is defined using surface temperature and freeze-up is defined using ice concentration.

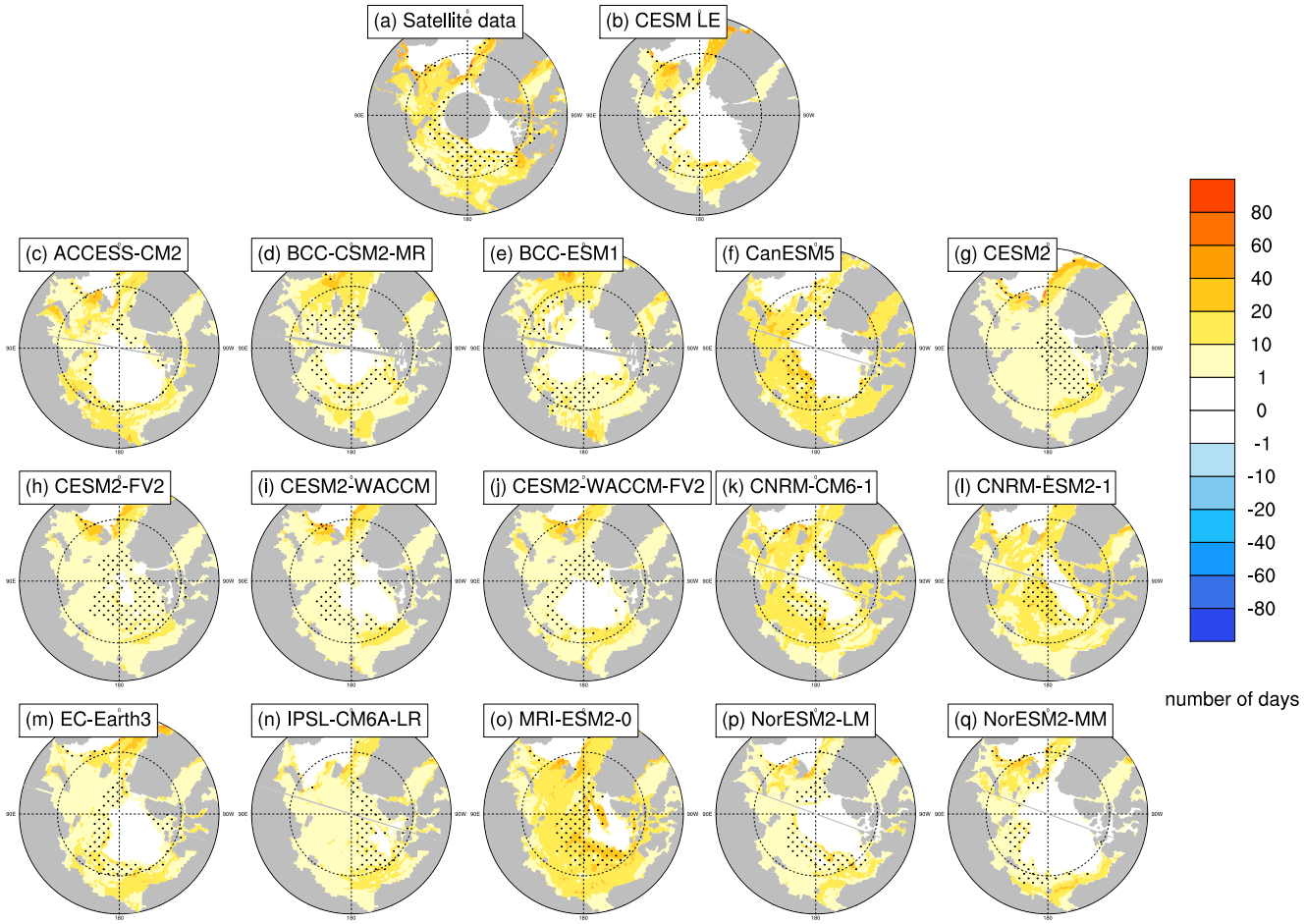

Figure S7. The length of the seasonal gain-of-ice period (number of days between freeze-up and closing) averaged over 1979–2014 at each grid cell using satellite data (a), the first ensemble member of the CESM LE (b) and the first ensemble member of each CMIP6 model (c-q). Stippling indicates where closing dates exist in less than 20% of years in the time range. Models on tripolar grids produce plot gaps filled by gray lines. No negative values are possible as both metrics are based on sequential ice concentration thresholds (15% and 80%).

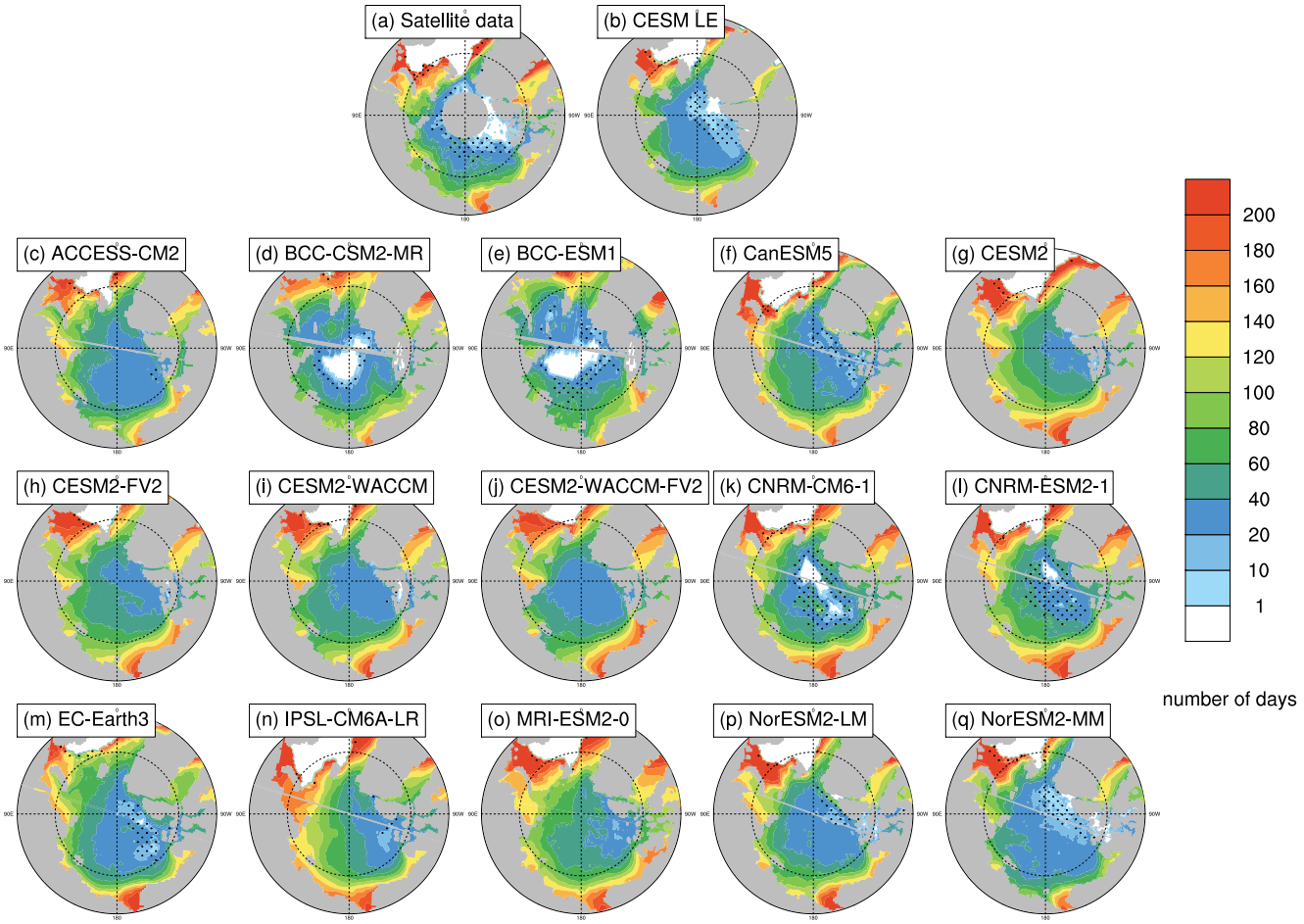

Figure S8. The length of the outer ice-free period (number of days between opening and closing, which use an 80% ice concentration threshold) averaged over 1979–2014 at each grid cell using satellite data (a), the first ensemble member of the CESM LE (b) and the first ensemble member of each CMIP6 model (c-q). Stippling indicates where closing dates exist in less than 20% of years in the time range. Models on tripolar grids produce plot gaps filled by gray lines.

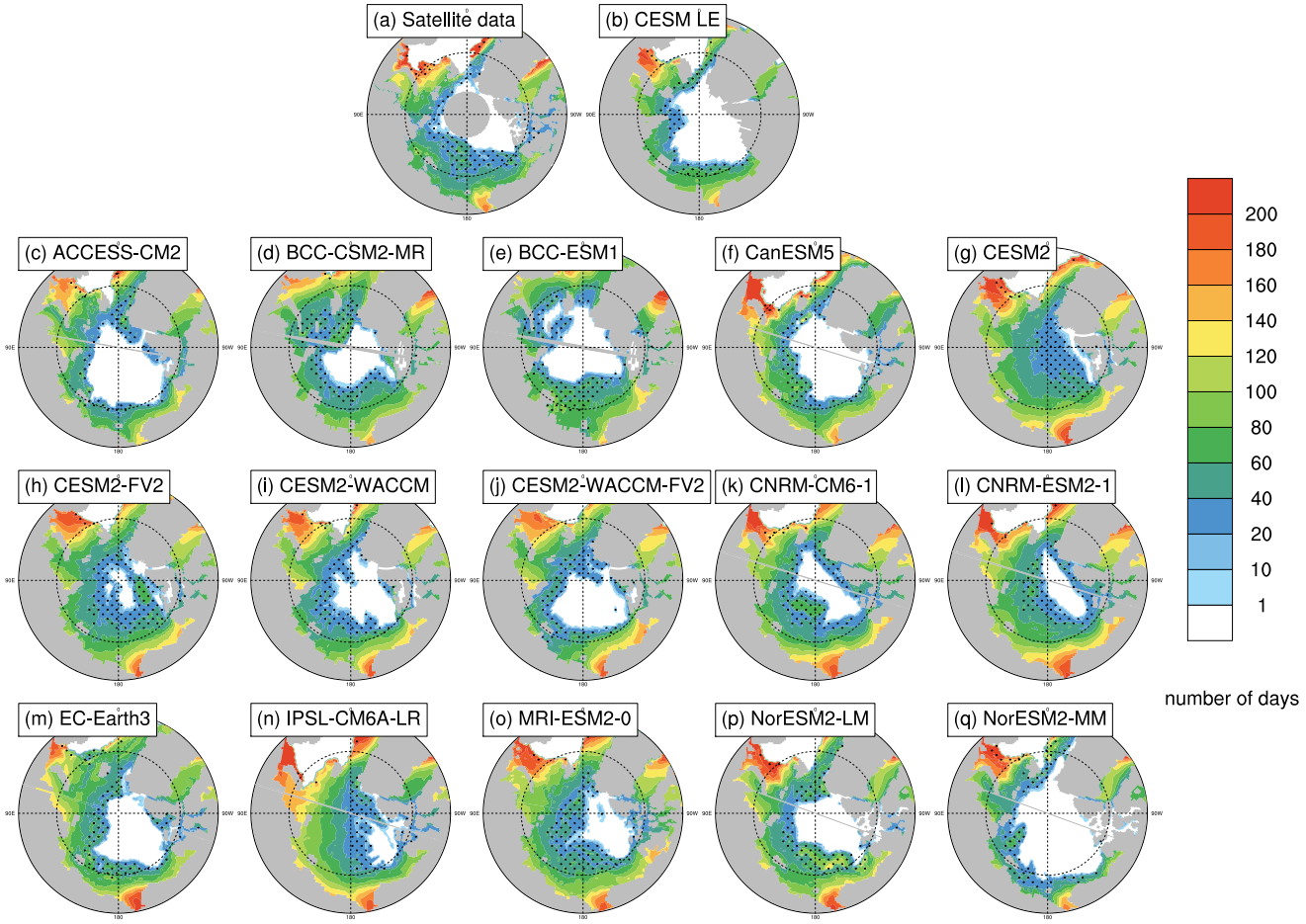

Figure S9. The length of the open water period (number of days between break-up and freeze-up, which use a 15% ice concentration threshold) averaged over 1979–2014 at each grid cell using satellite data (a), the first ensemble member of the CESM LE (b) and the first ensemble member of each CMIP6 model (c-q). Stippling indicates where closing dates exist in less than 20% of years in the time range. Models on tripolar grids produce plot gaps filled by gray lines.

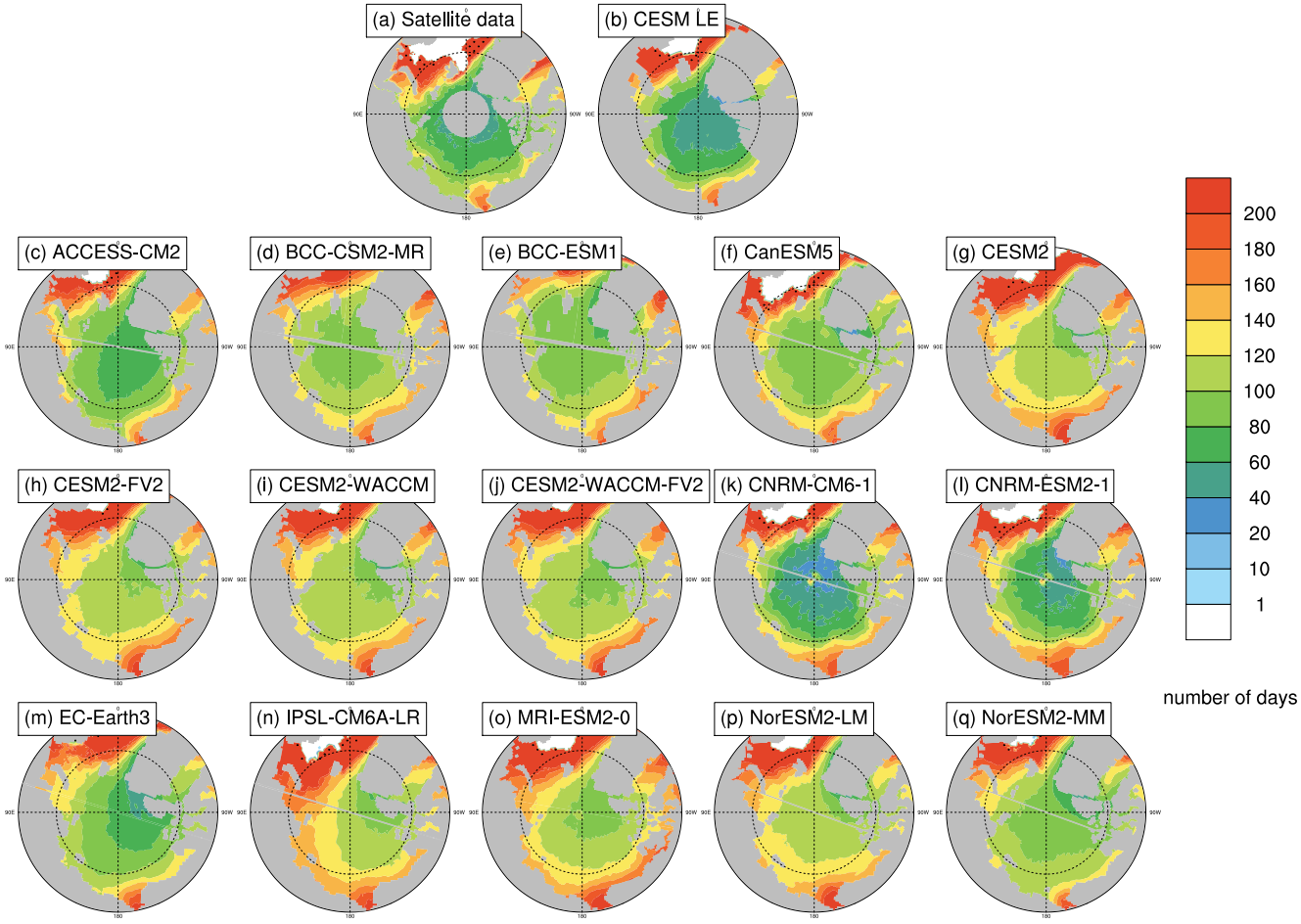

Figure S10. The length of the melt season (number of days between melt onset and freeze onset, which are defined using surface temperature in the models and brightness temperatures in the satellite data) averaged over 1979–2014 at each grid cell using satellite data (a), the first ensemble member of the CESM LE (b) and the first ensemble member of each CMIP6 model (c-q). Stippling indicates where closing dates exist in less than 20% of years in the time range. Models on tripolar grids produce plot gaps filled by gray lines.

	Melt onset	Opening (80%)	Break-up (15%)	Freeze onset	Freeze-up (15%)	Closing (80%)
ACCESS-CM2	**0.52**	**0.74**	0.24	**-0.76**	**-0.74**	**-0.67**
BCC-CSM2-MR	0.33	**0.46**	0.16	**-0.70**	**-0.47**	**-0.66**
BCC-ESM1	**0.55**	-0.16	0.05	**-0.69**	**-0.58**	**-0.47**
CESM2	**0.38**	**0.76**	0.30	**-0.82**	**-0.75**	**-0.86**
CESM2-FV2	**0.66**	**0.73**	0.09	**-0.85**	**-0.69**	**-0.74**
CESM2-WACCM	**0.53**	**0.65**	-0.07	**-0.73**	**-0.48**	**-0.67**
CESM2-WACCM-FV2	**0.49**	**0.67**	**0.36**	**-0.79**	**-0.67**	**-0.73**
CNRM-ESM2-1	**0.46**	-0.15	-0.11	-0.19	-0.13	-0.17
CNRM-CM6-1	0.19	-0.18	-0.11	-0.07	-0.04	-0.08
EC-Earth3	**0.75**	**0.53**	**0.48**	**-0.91**	**-0.82**	**-0.79**
MRI-ESM2-0	**0.37**	**0.46**	-0.18	**-0.83**	**-0.76**	**-0.79**
NorESM2-LM	**0.47**	**0.63**	0.03	**-0.68**	**-0.46**	**-0.61**
NorESM2-MM	**0.44**	0.08	**-0.47**	**-0.53**	**-0.4**	**-0.38**
CanESM5	**0.68**	**0.50**	**-0.11**	**-0.61**	**-0.54**	**-0.57**
IPSL-CM6A-LR	**0.42**	**0.49**	**-0.08**	**-0.78**	**-0.66**	**-0.71**
CESM LE	**0.35**	**0.19**	**-0.11**	**-0.76**	**-0.35**	**-0.43**

Table S5. As in Table 6, correlation coefficients (R-values) between seasonal sea ice transition dates but with summer (June–September) mean sea ice thickness of the same year instead of sea ice area from 1979–2014. Values in bold are statistically significant at the 95% confidence level. Correlation coefficients and p-values for models in the first thirteen rows are determined using one ensemble member, for CanESM5 using all 35 ensemble members, for IPSL using all 30 ensemble members and CESM LE using all 40 ensemble members. All values are calculated between 66-84.5°N.

	Melt onset	Opening (80%)	Break-up (15%)	Freeze onset	Freeze-up (15%)	Closing (80%)
ACCESS-CM2	-0.16	0.06	-0.15	0.00	-0.04	-0.06
BCC-CSM2-MR	**0.49**	0.25	0.29	**-0.41**	**-0.35**	**-0.43**
BCC-ESM1	0.29	-0.17	-0.19	**-0.36**	**-0.36**	**-0.43**
CESM2	0.06	**0.38**	0.15	-0.19	-0.22	**-0.25**
CESM2-FV2	**0.44**	**0.51**	0.14	**-0.69**	**-0.61**	**-0.60**
CESM2-WACCM	0.21	**0.42**	**0.41**	**-0.39**	**-0.50**	**-0.50**
CESM2-WACCM-FV2	**0.49**	**0.44**	0.22	**-0.64**	**-0.49**	**-0.52**
CNRM-ESM2-1	**-0.51**	**-0.49**	**-0.46**	**0.59**	**0.53**	**0.56**
CNRM-CM6-1	-0.09	-0.09	-0.28	-0.11	0.06	-0.08
EC-Earth3	**0.79**	**0.56**	**0.44**	**-0.84**	**-0.77**	**-0.75**
MRI-ESM2-0	0.29	**0.43**	0.08	**-0.53**	**-0.59**	**-0.53**
NorESM2-LM	-0.02	-0.07	0.18	0.18	0.03	0.05
NorESM2-MM	0.32	-0.2	-0.05	-0.19	**-0.35**	-0.12
CanESM5	**0.50**	**0.39**	0.04	**-0.64**	**-0.54**	**-0.52**
IPSL-CM6A-LR	**0.40**	**0.36**	**0.19**	**-0.39**	**-0.44**	**-0.40**
CESM LE	**0.12**	-0.02	-0.04	**-0.07**	**0.13**	**0.10**
Satellite data	**0.57**	**0.42**	**0.38**	**-0.61**	**-0.35**	**-0.48**

Table S6. As in Table 7, correlation coefficients (R-values) between seasonal sea ice transition dates but with March sea ice area instead of sea ice thickness from 1979–2014. Spring transition dates (melt onset, opening and break-up) are correlated with March mean ice area from the same year, while fall transition dates (freeze onset, freeze-up and closing) are correlated with March mean ice area from the following year. Values in bold are statistically significant at the 95% confidence level. Correlation coefficients and p-values for models in the first thirteen rows are determined using one ensemble member, for CanESM5 using all 35 ensemble members, for IPSL using all 30 ensemble members and CESM LE using all 40 ensemble members. All values are calculated between 66-84.5°N.

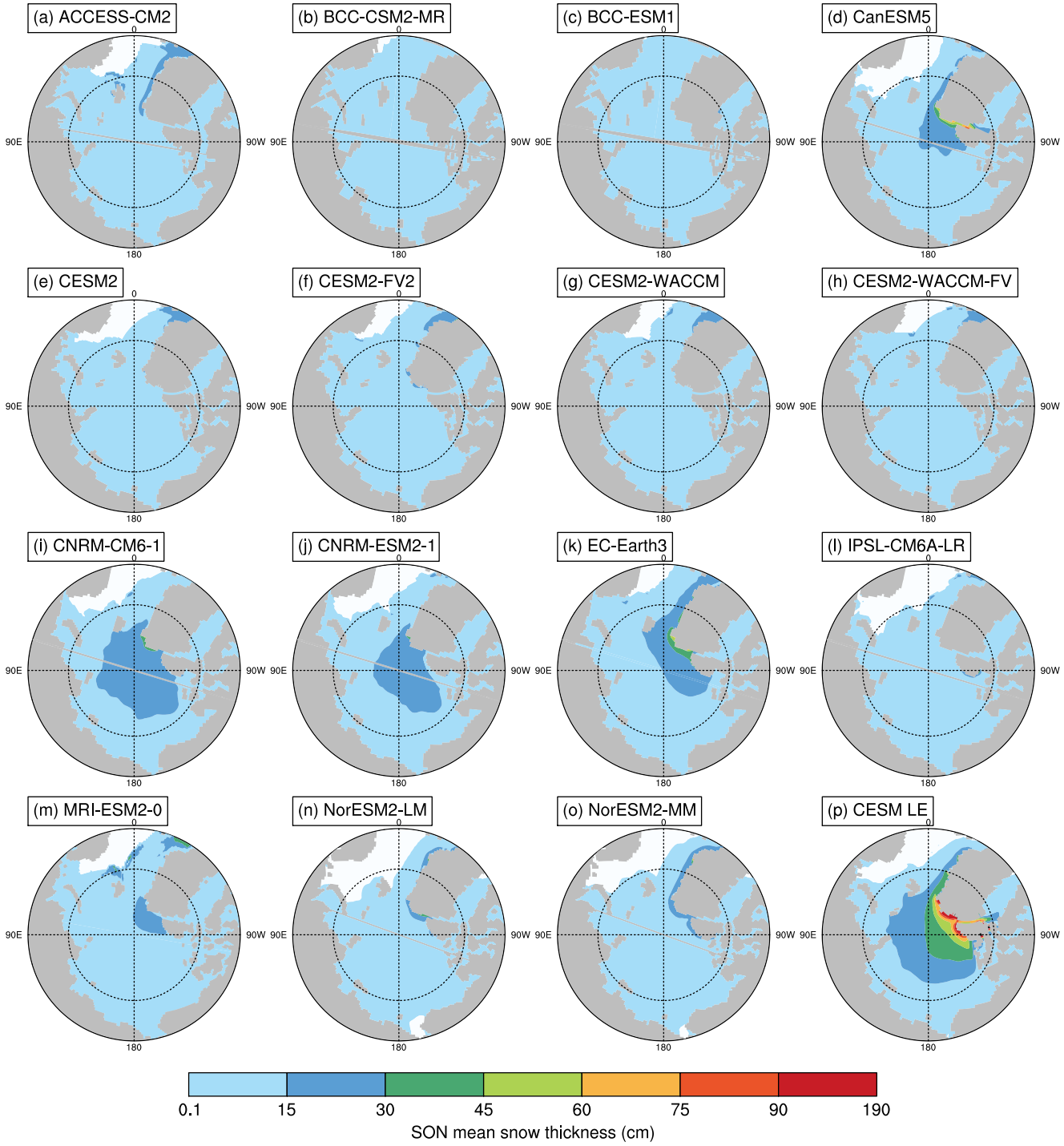

Figure S11. September–November mean snow thickness using the first ensemble member of each CMIP6 model (a-o) and the CESM LE (p) from 1979–2014. Note that the largest contour interval spans 100 cm instead of 15 cm to account for the very high snow depths in the CESM LE.

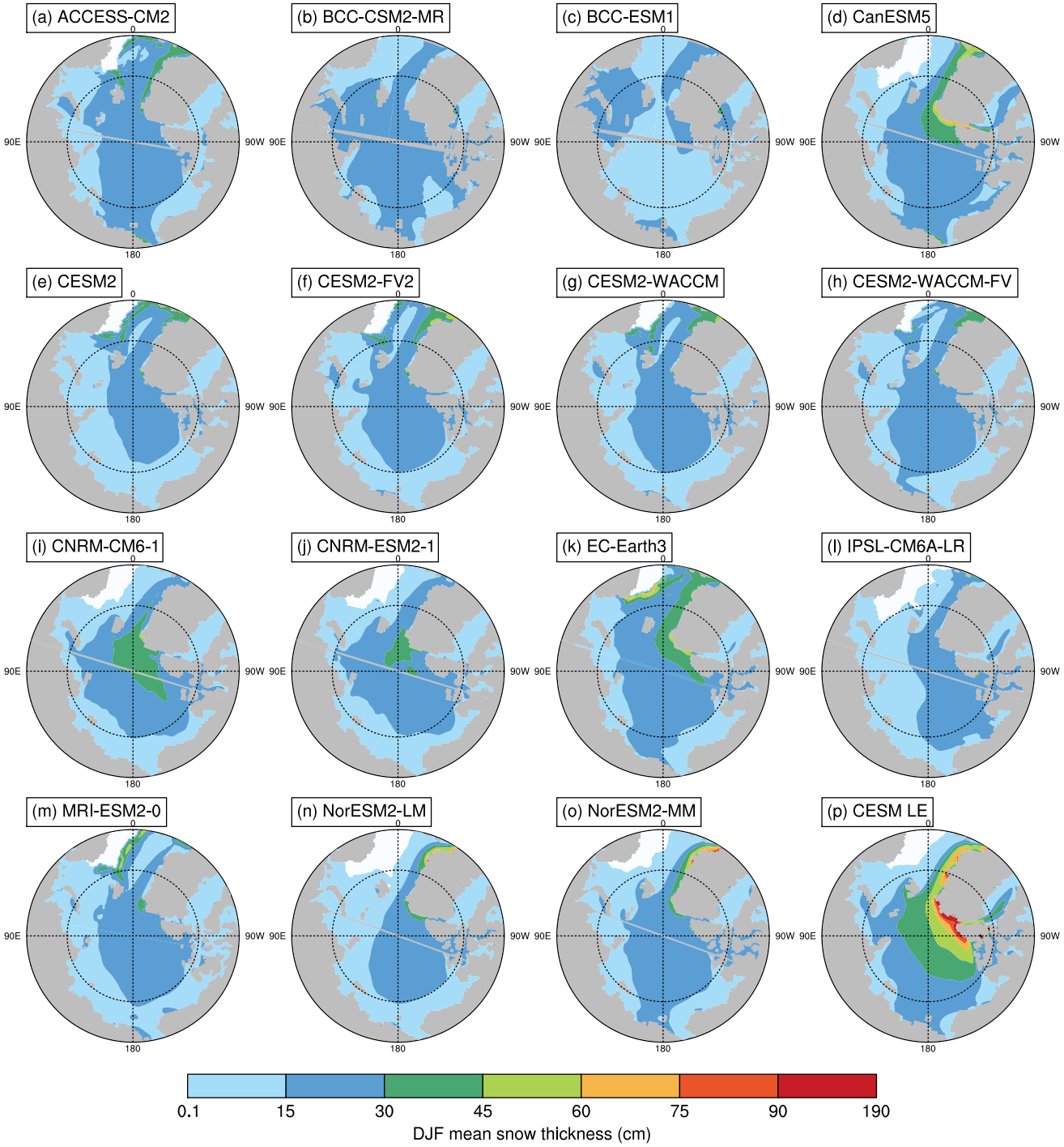

Figure S12. December–February mean snow thickness using the first ensemble member of each CMIP6 model (a-o) and the CESM LE (p) from 1979-2014. Note that the largest contour interval spans 100 cm instead of 15 cm to account for the very high snow depths in the CESM LE.